Available online at www.sciencedirect.com
ScienceDirect
Ceramics International 37 (2011) 979–984
CERAMICS INTERNATIONAL
www.elsevier.com/locate/ceramint

Dielectric and piezoelectric properties of rare-earth gadolinium modified lead lanthanum zirconium niobium titanate ceramics

Koduri Ramam [a,*], K. Chandramouli [b]

[a] Departmento de Ingenieria de Materials (DIMAT), Facultad de Ingenieria, Universidad de Concepción, Concepción, Chile
[b] Solid State Physics & Materials Research Labs., Department of Physics, Andhra University, Visakhapatnam, India

Received 2 August 2010; received in revised form 20 August 2010; accepted 3 November 2010
Available online 3 December 2010

Abstract

This paper reports the dielectric and piezoelectric properties of rare-earth Gd modified PLZNT solid solutions with a stoichiometric formula $[Pb_{(0.988-x)}La_{0.012}Gd_x][(Zr_{0.53}Ti_{0.47})_{(0.972-(x/4))}Nb_{0.02}O_3]$ (hereafter known as PLGZNT) with $x = 0$, 0.2, 0.4, 0.6, 0.8 and 1.0 mol% synthesized through solid state reaction method for phase formation, microstructure, dielectric and piezoelectric properties. The powder X-ray diffraction results obtained for PLGZNT ceramics showed pure perovskite phase with tetragonal symmetry sintered at 1245 °C supported by an accurate structure analysis of tolerance factor (t) and averaged electronegativity difference (e). The scanning electron micrograph showed pore-free homogeneous nature of grains which could be ascribed to a denser ceramics having enhanced distribution of grain orientations. It is observed that increasing Gd content in the lattice influenced the dielectric and piezoelectric properties. The optimum dielectric (ε_{RT} and tan δ) and piezoelectric properties (d_{33} and k_p) were observed in 0.6 mol% Gd modified PLZNT ceramic composition which attained saturation and thereafter decreased.

PACS : 77.84.−s; 77.70.+a; 77.90.+k; 77.84.Dy

Keywords: Perovskite; Ferroelectrics; X-ray diffraction; Dielectric response; Piezoelectricity

1. Introduction

The most important ferroelectric ceramics crystallize in the ABO_3 structured perovskite. The flexible structure of perovskite shows diverse physical properties which facilitates them interesting for functional applications [1,2]. Perovskites are perfect structures for fundamental research to better understand the cation and anion influence on structural and functional properties. The desired functional properties of polycrystalline solid solutions with perovskite structure can be tailored by either cationic modification or different synthesis routes [3]. The pure and modified structured perovskites have shown excellent electrical and mechanical properties and are ideal candidates for several ferroelectric and piezoelectric applications. When an asymmetrical crystal is subjected to a mechanical stress, it outputs a voltage whereas exhibits dimensional change when an electric field is applied. These two behaviors of crystal are referred as the direct and indirect modes of piezoelectric operation, respectively. Both modes of piezoelectric operation of perovskites are currently being utilized in many diverse applications [4,5]. La^{3+} modified at A-site in $Pb(Zr,Ti)O_3$ lattice known as $(Pb,La)(Zr,Ti)O_3$ is a well-known ferroelectric solid solution. PLZT has been extensively studied as it has interesting functional properties close to the morphotrophic phase boundary (MPB, Zr:Ti ≈ 52:48) on its phase diagram. The polycrystalline solid solutions of PLZT provide an excellent piezoelectric property after electrical poling [6].

The crucial step in PLZT fabrication is the final sintering process. It is essential to ensure that both excess PbO and deficit PbO can cause either PbO-rich grain boundaries; liquid phase sintering and unreacted phases or lead loss volatilization and excess lead vacancies with inconsistency in phase formation, respectively. Perovskite structured PLZT has been modified with many dopants such as Ag [7], Sm [8], Nd [9], Fe [10], Mn [11], Zn [12], Dy [13], Ce [14], and Yb [15]. The dopants will induce either oxygen (anion) or lead (cation) vacancies in the

* Corresponding author. Tel.: +56 41 2203369; fax: +56 41 2739800.
E-mail address: ramamk@udec.cl (K. Ramam).

0272-8842/$36.00
doi:10.1016/j.ceramint.2010.11.016

lattice due to either soft or hard doping influencing the properties. The morphotrophic phase boundary (MPB) is the point where the solid solution ceramic system at room temperature undergoes a morphotrophic phase transition in which the ferroelectric tetragonal structure transforms to a ferroelectric rhombohedral structure or vice versa depending on various factors such as Zr/Ti ratio, effect of dopants, and synthesis route. The dielectric and piezoelectric properties of PLZT doped with additives show anomalies near MPB. These anomalies are accountable for strong electromechanical behavior and make these solid solutions suitable for various applications. It is also known that pentavalent element Nb^{5+} (donor type) produces Pb vacancies (A-vacancy in ABO_3 perovskite) in PZT and enhances domain reorientation [16], resulting in high dielectric and piezoelectric properties.

We have been systematically studying either single or multiple soft and hard doping in PLZT lattice at different Zr/Ti ratios near MPB. However, the effect of rare-earth Gd substitution in the PLZT lattice for dielectric and piezoelectric properties is very limited. In this work, we investigated the dopant (Gd) influence on perovskite PLZNT to understand the mutual dependence of phase formation, stoichiometry, microstructure, physical and functional properties. The stoichiometric compositions of PLGZNT are given in Table 1.

2. Experimental

2.1. Ceramic processing

Analytical reagent grade (99.99% purity, Sigma–Aldrich, USA) PbO, La_2O_3, Gd_2O_3, ZrO_2, Nb_2O_5 and TiO_2 powders were mixed with excess 5 wt% (optimized) PbO to form PLGZNT (refer Table 1) as per stoichiometry. The batch powders were ball milled using zirconia balls and ethanol for 24 h. The dried powders were calcined at 950 °C for 3 h in an alumina crucible. Calcined powders were ball milled using zirconia balls and ethanol to obtain fine powders. The calcined fine powders were mixed with 5 wt% polyvinyl alcohol (PVA) as binder and were compacted into disk shaped samples sizing 12 mm in diameter and 2–3 mm thickness using steel die and hydraulic press under uniaxial pressure of 700–900 kg/cm^2. Binder was burned off at 500 °C for 2 h and sintered at 1245 °C for 3 h.

2.2. Structural characterization

The sintered specimens were characterized for phase formation by Philips X-ray diffractometer (PW-1710, CuK_α radiation, Ni filter, 1°/min). Scanning electron microscope (JEOL JSM 840A) was used to characterize microstructure of polished, etched and fractured ceramic surfaces. The apparent densities of sintered ceramics were measured using the Archimedes method.

2.3. Dielectric and piezoelectric characterization

Electroded ceramics were characterized for dielectric properties (ε_{RT}, ε_{Tc}, T_c and $\tan\delta$) by using HP-4192A Impedance Analyzer at 1 kHz. The dielectric constant is calculated from the following formula [1]:

$$\varepsilon = \frac{cd}{\varepsilon_0 A}$$

where c is capacitance, d is the thickness, A is the surface area of ceramic sample and ε_o = permittivity of free space = 8.85 - $\times 10^{-12}$ F/m. Electroded ceramics were poled in silicon oil bath at 100 °C by applying a dc field of 20 kV/cm. The piezoelectric charge coefficients (d_{33}) were characterized using a Berlincourt piezo-d-meter. The piezoelectric planar coupling coefficient (k_p) was characterized as follows: as per the IRE Standards on Piezoelectric Crystals: Measurements of Piezoelectric Ceramics, the following formula has been employed to find out piezoelectric planar coupling coefficient (k_p). The piezoelectric planar coupling coefficient was characterized as per the IRE Standards on Piezoelectric Crystals Measurements of Piezoelectric Ceramics: IRE Proceedings, 46, 764, 1958, the following formula being employed.

$$\frac{k_p^2}{1-k_p^2} = 2.51 \times \left[\frac{f_a - f_r}{f_r}\right]$$

where k_p: piezoelectric planar coupling coefficient, f_r: resonance frequency and f_a: anti-resonance frequency of poled ceramic samples. The resonance (f_r) and anti-resonance (f_a) frequencies of poled ceramics were measured by using a 4192A HP impedance analyzer.

Table 1
Stoichiometric PLGZNT ceramic compositions synthesized.

Formulae	
General formula	$[Pb_{(1-w-x)}La_wGd_x][(Zr_zTi_{1-z})_{(1-(w/4)-(x/4)-(5*k/4))}Nb_kO_3]$
PLGZNT	$[Pb_{(0.988-x)}La_{0.012}Gd_x][(Zr_{0.53}Ti_{0.47})_{(0.972-(x/4))}Nb_{0.02}O_3]$—(PLGZNT)
mol%	w = La = 1.2, z = Zr = 53, $1-z$ = Ti = 47, k = Nb = 2 and x = Gd = 0, 0.2, 0.4, 0.6, 0.8, and 1
0	$0.988PbO + 0.006La_2O_3 + 0.51516ZrO_2 + 0.45684TiO_2 + 0.01Nb_2O_5 \rightarrow [Pb_{0.988}La_{0.012}Gd_0][Zr_{0.53}Ti_{0.47}]_{(}\Delta^B{}_{0.972)}Nb_{0.02}O_3$
0.2	$0.986PbO + 0.006La_2O_3 + 0.001Gd_2O_3 + 0.514895ZrO_2 + 0.456605TiO_2 + 0.01Nb_2O_5 \rightarrow [Pb_{0.986}La_{0.012}Gd_{0.002}][Zr_{0.53}Ti_{0.47}]_{(}\Delta^B{}_{0.9715)}Nb_{0.02}O_3$
0.4	$0.984PbO + 0.006La_2O_3 + 0.002Gd_2O_3 + 0.51463ZrO_2 + 0.45637TiO_2 + 0.01Nb_2O_5 \rightarrow [Pb_{0.984}La_{0.012}Gd_{0.004}][Zr_{0.53}Ti_{0.47}]_{(}\Delta^B{}_{0.971)}Nb_{0.02}O_3$
0.6	$0.982PbO + 0.006La_2O_3 + 0.003Gd_2O_3 + 0.514365ZrO_2 + 0.456135TiO_2 + 0.01Nb_2O_5 \rightarrow [Pb_{0.982}La_{0.012}Gd_{0.006}][Zr_{0.53}Ti_{0.47}]_{(}\Delta^B{}_{0.9705)}Nb_{0.02}O_3$
0.8	$0.980PbO + 0.006La_2O_3 + 0.004Gd_2O_3 + 0.51410ZrO_2 + 0.45590TiO_2 + 0.01Nb_2O_5 \rightarrow [Pb_{0.980}La_{0.012}Gd_{0.008}][Zr_{0.53}Ti_{0.47}]_{(}\Delta^B{}_{0.97)}Nb_{0.02}O_3$
1	$0.978PbO + 0.006La_2O_3 + 0.005Gd_2O_3 + 0.513835ZrO_2 + 0.455665TiO_2 + 0.01Nb_2O_5 \rightarrow [Pb_{0.978}La_{0.012}Gd_{0.01}][Zr_{0.53}Ti_{0.47}]_{(}\Delta^B{}_{0.9695)}Nb_{0.02}O_3$

3. Results and discussion

3.1. XRD characterization

Fig. 1 depicts X-ray diffraction patterns of Gd modified lead lanthanum zirconium niobium titanate (designated as PLGZNT) ceramics. All the XRD patterns were found to have single phase with tetragonal structure. XRD studies revealed that Gd^{3+} doping at A-site of PLZNT lattice resulted in enhanced tetragonality. It can be seen that the peaks of the (0 0 2) and (2 0 0), (1 0 2) and (2 0 1), (1 1 2) and (2 1 1) planes correspond to tetragonal symmetry. It is reported that Gd^{3+} with smaller ionic radius (0.93 Å) similar to that of Zr^{4+}/Ti^{4+} = 0.72 Å/0.605 Å enters B-site [17] while Gd^{3+} ions having higher ionic radius (1.107 Å) occupy the A-sites which is similar to that of Pb^{2+} = 1.49 Å. It is reported that the vacancies could exist at both A and B sites in PLZT lattice [18]. In our study, it is expected that Gd^{3+} (1.107 Å) occupies A-site and creates vacancies on B-site due to the approximately similar ionic radii of Pb^{2+} (1.49 Å) and La^{3+} (1.36 Å) at A-site. Shannon [20] reported that the ionic radii of Gd^{3+} with 6 fold coordination is 0.93 Å whereas the ionic radii of Gd^{3+} with 9 fold coordination is 1.107 Å.

The substitution of La^{3+} and Gd^{3+} ions on the Pb^{2+} lattice sites were charge compensated by the formation of V_B'''' small cationic vacancies on the Zr/Ti lattice sites. The trivalent ions La^{3+} and Gd^{3+} partially substitute Pb^{2+} and cationic vacancies are created on B-site.

3.2. Tolerance factor and electronegativity

The perovskite structure with A (large cations), B (small cations) and O (anions) can be characterized by the tolerance factor *t*. According to Goldschmidt, a perovskite is stable only if a tolerance factor, *t*, falls in between $0.8 < t < 0.99$ and beyond this range indicates distortion in perovskite structure [19]. The stability of the perovskite can be ascertained by both tolerance factor (*t*) and averaged electronegativity difference (*e*), respectively. The tolerance factor and averaged electronegativity difference have been calculated using the effective ionic radii [20] and revised Pauling's electronegativity, respectively. The tolerance factor (*t*) can be calculated as follows using the ionic radii of large (r_A) and small cations (r_B) and (r_O) of anions [6]:

$$t = \frac{r_A + r_O}{\sqrt{2}(r_B + r_O)}$$

By and large, the stability of the crystal structure can also be characterized by averaged electronegativity difference. Besides, using the tolerance factor, *t*, to classify the perovskite structure, the average electronegativity can be calculated as [6]:

$$e = \frac{(\chi_A - \chi_O) + (\chi_B - \chi_O)}{2}$$

In the above expression, the individual electronegativities of A and B-cations, and O-anions are represented by χ_A, χ_B and χ_O, respectively. By using the stoichiometric chemical equation for the perovskite system, the averaged electronegativity difference (*e*) can be written as:

$$e = \frac{(0.988-x)\chi_{Pb-O}+0.012\chi_{La-O}+x\chi_{Gd-O}+[(0.972-(x/4))(0.53\chi_{Zr-O}+0.47\chi_{Ti-O})]+0.02\chi_{Nb-O}}{1.992-(x/4)}$$

Table 2 shows the tolerance factor (*t*) and averaged electronegativity difference (*e*) of PLGZNT ceramics. In our study, the calculated tolerance factor (*t*) values of tetragonal structured PLGZNT ceramics fall within the perovskite range and showed a consistent trend with a slight variation of 0.0001 in *t* values supporting the tetragonal perovskite. Concurrently, the averaged electronegativity difference (*e*) of tetragonal structured PLGZNT ceramics showed a consistent trend with a slight variation of 0.001 in *e* values that characterize tetragonal perovskite lattice.

3.3. Microstructure and apparent density

Fig. 2 depicts scanning electron micrographs of fractured surface of Gd modified PLZNT ceramics, respectively. The grains were homogenous in nature and the grain growth increased as Gd content increased up to 0.6 mol%. The grain growth inhibition at 1 mol% Gd can be ascribed to the grain-boundary pinning process induced by the own presence of

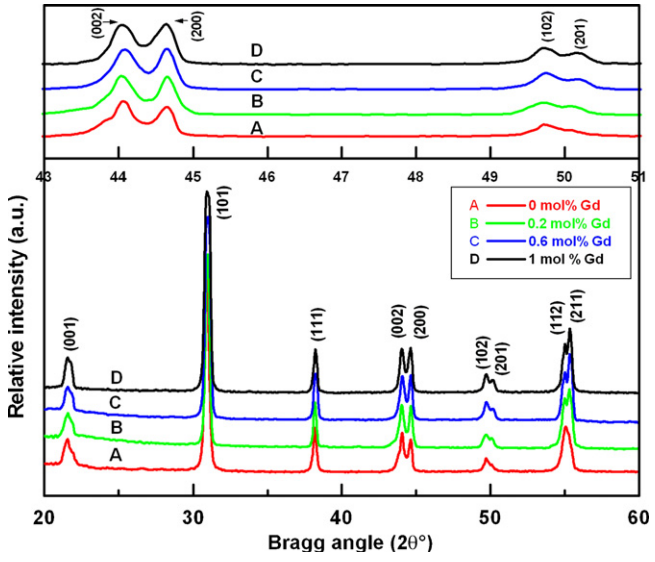

Fig. 1. X-ray diffraction patterns of Gd modified PLZNT ceramics.

Table 2
Tolerance factor (*t*) and averaged electronegativity difference (*e*) of PLGZNT ceramics.

Gd (mol%)	Tolerance factor (*t*)	Averaged electronegativity difference (*e*)
0	0.8276	1.564
0.2	0.8276	1.565
0.4	0.8275	1.566
0.6	0.8275	1.567
0.8	0.8274	1.568
1.0	0.8274	1.569

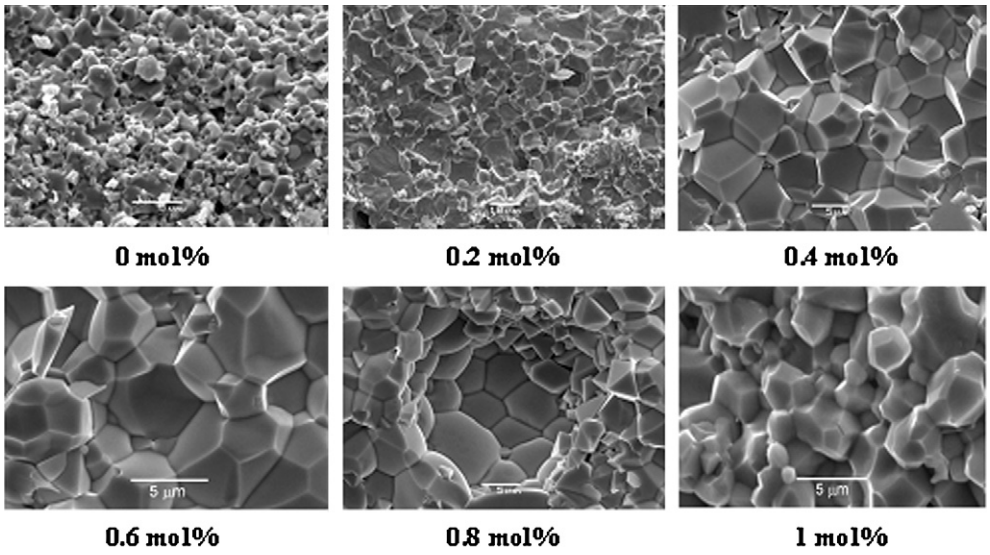

Fig. 2. Scanning electron micrographs (fractured surface) of Gd modified PLZNT ceramics.

(substitutional and/or interstitial) Gd, which resulted in inhibited grain growth. The grain growth increment could be attributed to the different dopants (La^{3+}, Gd^{3+} and Nb^{5+}) at the grain boundaries and lead vacancies caused by the dopants whereas the grain growth inhibition could have been caused by the excess Gd ions stagnating at the grain boundaries hindering the mobility. The pore-free homogenous grains can be evidenced from the fractured scanning electron micrograph. In general, after attaining saturation, the Lanthanide ions increasingly inhibit grain growth as their atomic numbers increase. In our study, we observed a grain growth up to 0.6 mol% Gd after which grain growth inhibited. A similar decrease in grain growth has been reported [21]. Fig. 3 shows apparent density of Gd modified PLZNT ceramics. In our study, it is observed that the density showed an increasing trend till 0.6 mol% Gd doped PLZNT ceramic. This could be accredited to the homogeneous grains without pores due to two trivalent ions at A-site in the PLGZNT lattice. The maximum density can be observed in 0.6 mol% (7.724 gm/cm^3) PLGZNT ceramic.

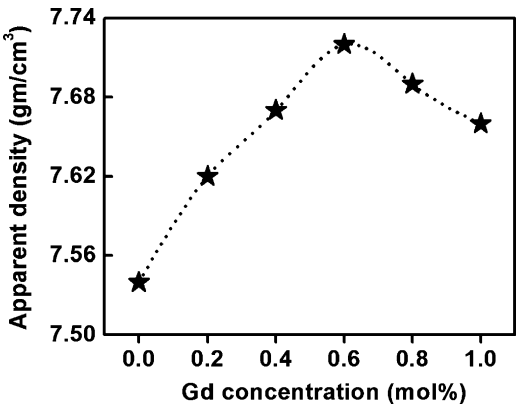

Fig. 3. Apparent density of Gd modified PLZNT ceramics.

3.4. Dielectric characterization

Fig. 4(i–iv) shows temperature dependent dielectric properties of Gd modified PLZNT ceramics at 1 kHz, respectively. Dielectric studies indicated that room temperature dielectric response enhanced ($\varepsilon_{RT} = 2342$) up to 0.6 mol% Gd which could be due to the enhanced electric-dipole polarization in the PLGZNT lattice. When compared to the undoped, the dielectric constant of PLGZNT ceramics increased rapidly and reached a maximum at 0.6 mol% Gd. Further Gd doping resulted in decrement of dielectric constant due to the non-diffusion of excess Gd in the ceramics. As Gd content increased, the Curie temperature (331–253 °C) and dielectric loss showed a decreasing trend while the dielectric maximum ($\varepsilon_{Tc} = 23{,}108$) increased constantly throughout the series. The dielectric properties of PLZT ceramics are known to depend on the grain growth and density of the ceramics. Okazaki and Nagata [22] have observed that, in PLZT ceramics (La:Zr:Ti = 48:65:35), T_c increases and K_{max} decreases with decreasing grain growth. In our study, we chose the solid solutions with La:Zr:Ti = 1.2/53:47 near morphotrophic phase boundary having a tetragonal symmetry. The grain growth and density showed increasing tendency resulting in enhanced dielectric constant and dielectric maximum whereas the Curie temperature and dielectric loss decreased. An increase in tetragonality is one of the reasons for the increased dielectric constant. An inverse dependence of grain growth on T_c and K_{max} has been reported [23]. Moreover, Gd^{3+} and La^{3+} both occupied at A-site in PLGZNT lattice due to the approximately similar ionic radii and vacancies created in the B-site. Thus, the charge compensation occur by the creation of vacancies at B-site and as Gd content increased the polarization also increased and attained saturation at 0.6 mol% Gd reaching the solid solubility limit which is not comparable with PLNZNT [9] (Table 3).

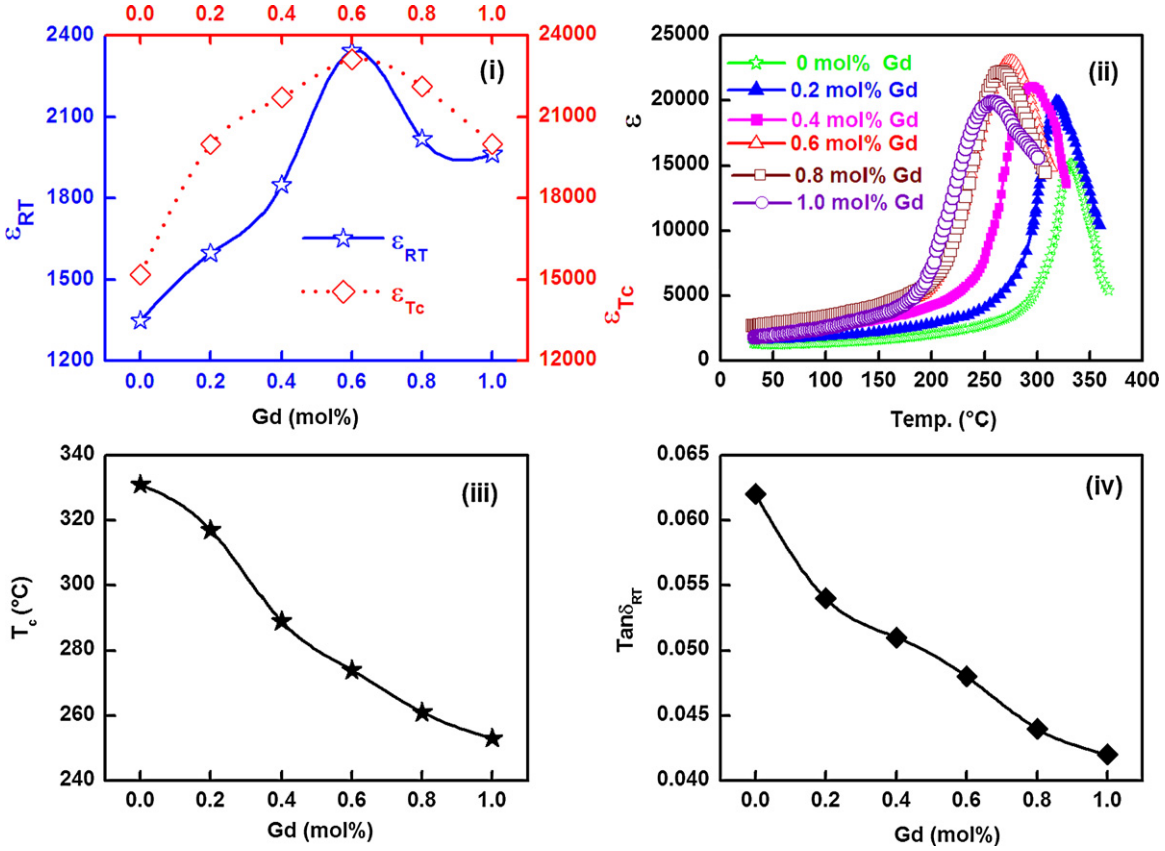

Fig. 4. (i–iv) Temperature dependent dielectric properties of Gd modified PLZNT ceramics at 1 kHz, respectively.

3.5. Piezoelectric characterization

Fig. 5 shows the piezoelectric charge coefficient (d_{33}) and piezoelectric planar coupling coefficient (k_p) of Gd modified PLZNT ceramics, respectively. It is observed that d_{33} and k_p enhanced with increasing Gd content up to 0.6 mol%. The dielectric and piezoelectric properties showed a dependence on the amount of Gd content in the ceramic compositions. The piezoelectric properties both piezoelectric charge coefficient (d_{33} = 574 pC/N) and electromechanical planar coupling coefficient (k_p = 0.589) for PLGZNT system increased with the increasing Gd content up to 0.6 mol% and thereafter decreased. The substitution of cations in a perovskite lattice, i.e. Pb^{2+}, La^{3+}, Zr^{4+} and Ti^{4+} are replaced partially by cations (Gd^{3+} at A-site) and (Nb^{5+} at B-site) with similar ionic radii as those of the replaced ions, respectively. In the case of tetragonal PZT ceramics, 50% of the domains perpendicular to the applied field can be reoriented by poling and about 44% of them are maintained after removing the poling field. The internal stains (or stresses) are gradually removed in the course of time by domain motion (by new domain nucleation, domain splitting and domain wall displacement). The piezoelectric properties strongly depend on the grains and dopant concentrations as well as MPB region. The Gadolinium causes significant changes as the trivalent rare-earth ions have distinct properties depending on several factors. The enhanced piezoelectric properties were attained due to the high densification along with homogeneous grains contributed the piezoelectric effect. The higher content of Gd resulted in lower piezoelectric properties could be attributable to the non-diffusivity of excess Gd ions and could expect defects within the domain. As the Gd content increased,

Table 3
Ionic radii of elements in PLGZNT ceramics [20].

Elements	Ionic radii	Fold
Pb^{2+}	1.49	12
La^{3+}	1.36	12
Gd^{3+}	1.107	9
Zr^{4+}	0.72	6
Ti^{4+}	0.605	6
Nb^{5+}	0.64	6
O^{2-}	1.4	6

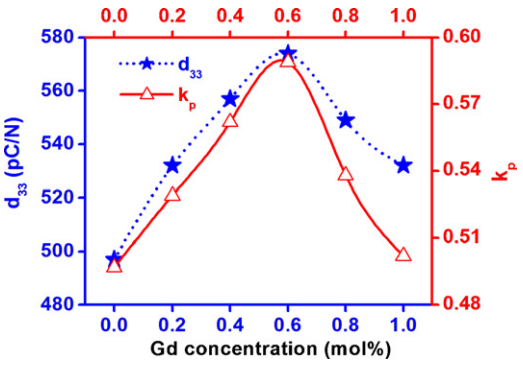

Fig. 5. Piezoelectric properties of Gd modified PLZNT ceramics.

the Pb vacancies also increased and at higher concentrations the defects occur reducing the electrical properties. Maximum values of d_{33} (574 pC/N) and k_p (0.589) are found in 0.6 mol% Gd doped PLZNT ceramic. The d_{33} and k_p reported in this series are larger than those of earlier studies [24–26].

4. Conclusion

In conclusion, the perovskite structured $[Pb_{(0.988-x)}La_{0.012}Gd_x][(Zr_{0.53}Ti_{0.47})_{(0.972-(x/4))}Nb_{0.02}O_3]$ solid solutions have been synthesized through solid state reaction route. X-ray diffraction patterns of PLGZNT with peak splittings of (0 0 2) and (2 0 0), (1 0 2) and (2 0 1), (1 1 2) and (2 1 1) correspond to ferroelectric tetragonal phase. The calculated tolerance factor (t) and averaged electronegativity difference (e) values of PLGZNT ceramics confirmed the tetragonal perovskite symmetry. The homogeneous microstructure could be credited to grains without pores and two trivalent ions at A-site in the PLGZNT lattice which promoted the density till 0.6 mol% Gd. Dielectric constant at room temperature enhanced up to 0.6 mol% Gd along with dielectric maximum whereas Curie temperature and dielectric loss continuously decreased. The piezoelectric properties (d_{33} and k_p) enhanced due to the presence of two trivalent cations at A-site in the perovskite and increasing Gd content contributed considerably to the piezoelectric effect. Among the series, 0.6 mol% Gd showed optimum dielectric and piezoelectric properties. In our study, the advantages of Gd modified PLZNT showed improved properties of density, dielectric constant (ε_{Tc}), piezoelectric properties (d_{33}, k_p) with low T_c and tan δ_{RT} up to 0.6 mol% than PLZNT. The main disadvantage of Gd modified PLZNT is higher concentrations of Gd led to deterioration of properties.

Acknowledgements

The authors would like to acknowledge University of Concepcion, Chile and Andhra University, India. We would also like to thank Ms. C.N. Devi, Mr. Ranganathan and Mr. Krishnamurthy for their technical support extended during this work.

References

[1] B. Jaffe, W.R. Cook Jr., H. Jaffe, Piezoelectric Ceramics, Academic Press Inc., London, 1971.
[2] G.H. Haertling, Piezoelectric and electrooptic ceramics, in: R.C. Buchanan (Ed.), Ceramic Materials for Electronics, Marcel Dekker Inc., New York, 1986, pp. 139–225.
[3] H. Beltran, E. Cordoncillo, P. Escribano, J.B. Carda, A. Coats, A.R. West, Chem. Mater. 12 (2000) 400.
[4] E.F. Crawley, AIAA J. 32 (8) (1994) 1689.
[5] S.S. Rao, M. Sunar, Appl. Mech. Rev. 47 (4) (1994) 113.
[6] Y. Xu, Ferroelectric Materials and their Applications, North-Holland, Amsterdam, 1991.
[7] G.H. Maher, J. Am. Ceram. Soc. 66 (6) (1983) 408.
[8] C. Prakash, O.P. Thakur, Mater. Lett. 57 (2003) 2310.
[9] K. Ramam, M. Lopez, J. Alloys Compd. 466 (1–2) (2008) 398.
[10] K. Ramam, M. Lopez, Phys. Stat. Sol. (a) 203 (15) (2006) 3852.
[11] J.J. Choi, S.W. Kim, H.E. Kim, J. Am. Ceram. Soc. 85 (3) (2002) 733.
[12] K. Ramam, M. Lopez, K. Chandramouli, Philos. Mag. Lett. 88 (6) (2008) 429.
[13] T.J. Boyle, P.G. Clem, B.A. Tuttle, G.L. Brennecka, J.T. Dawley, M.A. Rodriguez, T.D. Dunbar, W.F. Hammetter, J. Mater. Res. 17 (4) (2002) 871.
[14] K. Ramam, K. Chandramouli, Curr. Appl. Phys. 9 (5) (2009) 907.
[15] T.B. Queiroz, D. Mohr, H. Eckert, A.S.S. de Camargo, Solid State Sci. 11 (8) (2009) 1363.
[16] N. Vittayakorn, G. Rujijanagul, D.P. Cann, J. Alloys Compd. 440 (1–2) (2007) 259.
[17] J.A. Dean, Lange's Handbook of Chemistry, 13th edn., McGraw Hill, New York, 1985.
[18] K.H. Hardtl, D. Hennings, J. Am. Ceram. Soc. 55 (5) (1972) 20.
[19] F.S. Galasso, Structure, Properties and Preparation of Perovskite-type Compounds, Pergamon Press, Oxford, 1969.
[20] R.D. Shannon, Acta Crystallogr. A32 (1976) 751.
[21] P. Gonnard, M. Troccaz, J. Solid State Chem. 23 (1978) 321.
[22] K. Okazaki, K. Nagata, J. Am. Ceram. Soc. 56 (2) (1973) 82.
[23] H.B. Park, C.Y. Park, Y.S. Hong, K. Kim, S.J. Kim, J. Am. Ceram. Soc. 82 (1) (1999) 94.
[24] R.P. Tandon, V. Singh, R. Singh, N. Narayana Swami, Mater. Lett. 20 (3–4) (1994) 165.
[25] B. Sahoo, V.A. Jaleel, P.K. Panda, Mater. Sci. Eng. B126 (2006) 80.
[26] S.K.S. Parashar, R.N.P. Choudhary, B.S. Murty, Mater. Sci. Eng. B110 (2004) 58.